

Exploring the possible origin of spin reorientation transition in NdCrO₃

Hena Das,^{1,2,*} Alejandro F. Rébola,³ and Tanusri Saha-Dasgupta⁴

¹Laboratory for Materials and Structures, Tokyo Institute of Technology,
4259 Nagatsuta, Midori-ku, Yokohama 226-8503, Japan

²Tokyo Tech World Research Hub Initiative, Institute of Innovative Research,

Tokyo Institute of Technology, 4259 Nagatsuta, Midori-ku, Yokohama 226-8503, Japan

³Instituto de Física Rosario - CONICET, Bv. 27 de Febrero 210 bis, S2000EKF Rosario, Santa Fe, Argentina

⁴Department of Condensed Matter Physics and Material Sciences,
S. N. Bose National Centre for Basic Sciences, JD Block,
Sector III, Salt Lake, Kolkata, West Bengal 700106, India

(Dated: October 7, 2021)

Spin reorientation transitions and other related magnetic phenomena, which owe their origin to the complex interplay between multiple magnetic sublattices, have long attracted scientific attention both from the perspective of fundamental curiosity and technological applications. In this study, combining first principles calculations together with finite temperature Monte Carlo simulations, we explore the possible origins of reorientation transition of Cr spins in NdCrO₃. We construct a NdCrO₃ specific magnetic model, consisting of symmetric superexchange interactions between magnetic ions, as well as their magnetic anisotropy. We show that the observed spin reorientation in NdCrO₃, arises out of a delicate balance between Nd–Cr magnetic exchange interactions, single ion anisotropy of Nd spins, and single ion anisotropy of Cr spins. Moreover, though our model does not take into consideration the effect of anti-symmetric and anisotropic-symmetric magnetic exchanges, the qualitative as well as quantitative agreement of the theoretically derived and the experimentally observed spin-reorientation transition in NdCrO₃, confirms the merit of our proposed microscopic model. Our results also propose a hitherto unobserved collective magnetic ordering in Nd sublattice, which is challenging to detect as it is an extreme low temperature phenomena, therefore calls for further investigations.

PACS numbers:

INTRODUCTION

When multiple magnetic sublattices are formed in a perovskite structure, strong mutual interactions between these superlattices lead to unique magnetic and related phenomena [1–9]. The formation of these magnetic sublattices can be attributed to many factors, such as, certain chemical compositions [10, 11] or the formation of unique charge-ordered states [9]. In this regard, systems belonging to the rare-earth (R) transition metal (M) perovskite family, particularly RFeO₃ orthoferrites and RCrO₃ orthochromites, exhibit a rich variety of magnetic properties resulting from the interplay of two different magnetic sublattices. These systems crystallize in the orthorhombic *Pbnm* structure. Though the magnetic properties of RCrO₃ compounds are similar to those of the isomorphic RFeO₃ ones, the former group exhibits a wider range of magnetic phase transitions depending on the characteristic features of the associated rare-earth ions [12, 13]. The transition metal ordering temperatures are smaller by a factor ranging from two to six in the orthochromites compared to orthoferrites. For example, the M ordering temperature of NdFeO₃ is 690 K [14] as compared to that of NdCrO₃, which is reported to be 220 K [15]. This implies weaker M-M interaction in chromites compared to ferrites. Therefore, the M-M interaction in chromites is expected to strongly compete with the other magnetic interactions, such as R-M and R-R interactions. Subtle changes in the relative strength of these magnetic interactions can therefore influence the nature of magnetic behavior. Here, we are interested in NdCrO₃,

a system which was reported to show multiple phase transitions. However, the microscopic origin of these phenomena is yet to be deciphered. Moreover, for this system the magnitude of the rare-earth transition metal coupling is believed to be at least twice as large compared to its orthoferrite counterpart [16]. This phenomenon is also conjectured to influence the observed multiple phase transitions. However, the underlying microscopic mechanism is still unknown.

At high temperature, RMO₃ compounds are predominantly G-type antiferromagnets with small canting which results in weak ferromagnetism [17, 18]. A prominent phenomena in RMO₃ compounds is the spin reorientation (SR) [4, 13], in which as the temperature is lowered, the direction of the easy axis of the M sublattice magnetization changes from one crystal axis to another. Depending on the direction of the magnetization axis before and after the SR, six different groups can be identified: [12] (I) $G_x \rightarrow G_z$, (II) $G_x \rightarrow G_y$, (III) G_x , no SR (IV) G_y , no SR, (V) $G_z \rightarrow G_y$ (VI) G_z with a non-magnetic R atom, no SR, where x , y and z subscripts refer to easy-axis directions pointing to crystallographic a , b and c directions, respectively. In case of RCrO₃, system corresponds to R= Ce, Sm or Gd belong to category (I); R = Er belongs to category (II); R= Y, La or Eu belong to category (III); R = Tb, Dy, Ho, Yb, Pr or Tm belong to category (IV); R = Nd belongs to category (V); and R = Lu belongs to category (VI). By contrast, the ferrite series show less variety: system corresponds to R = Pr, Nd, Sm, Tb, Ho, Er, Tm or Yb belong to category (I); for R = Ce or Dy belong to category (II); and for R = Y, La, Eu or Lu belong to category (III); in support of the

fact that magnetism in chromites is more intricate and diverse compared to ferrites.

The magnetic properties of orthochromites and orthoferrites have been studied employing a variety of techniques, namely neutron diffraction and inelastic scattering [19, 20], bulk magnetization and susceptibility measurements on powders and single crystals [21], specific-heat studies on powders and single crystals [16, 22], Mossbauer effect [23], and optical-absorption spectroscopy [24]. In comparison, the theoretical studies are limited.

Within these systems, there are three types of magnetic interactions, $M^{3+}-M^{3+}$, $M^{3+}-R^{3+}$ and $R^{3+}-R^{3+}$, which according to their relative strengths set the following hierarchy: $M^{3+}-M^{3+} > M^{3+}-R^{3+} > R^{3+}-R^{3+}$ [12]. Each of these interactions generally consist of the isotropic, anti-symmetric and the anisotropic-symmetric superexchange interactions, apart from the single ion anisotropy of the M^{3+} and R^{3+} ions. This inevitably makes the theoretical study of magnetic properties of RMO_3 far from trivial. The most exhaustive study in this respect was carried out by Yamaguchi [12] in 1974 which employs first-order perturbation together with mean-field decoupling to study the spin-reorientation phenomenon in orthochromites and orthoferrites. In this work, the SR phenomena was investigated in the parameter space of a model Hamiltonian comprising of isotropic, anti-symmetric and the anisotropic-symmetric $M^{3+}-M^{3+}$, $M^{3+}-R^{3+}$ superexchange interactions, and the single-ion anisotropy of the M^{3+} ions. The magnetism of R sublattice was neglected, apart from M-R interaction. While this approach could explain the SR phenomena belonging to category (I) ($G_x \rightarrow G_z$) and category (II) ($G_x \rightarrow G_y$) highlighting role of anti-symmetric and anisotropic-symmetric $M^{3+}-R^{3+}$ interactions in SR of category (I) and category(II), the SR $G_z \rightarrow G_y$ (category (V)), as observed in $NdCrO_3$, could not be explained.

The possible cause for the failure of this theory in explaining SR in category (V), involving Nd-chromites, was speculated to be the single-ion anisotropy of Nd^{3+} , which was neglected in the theory by Yamaguchi [12], thus leaving the SR in $NdCrO_3$ unsolved. While the anisotropy energy of Gd^{3+} ion is small enough to be neglected, and that of Dy^{3+} is large enough to be treated as an Ising spin, the anisotropy energy of Nd^{3+} is intermediate between the two. This may have an important influence in deciding SR in Nd chromites when the Nd-Cr interaction is not negligible. To the best of our knowledge, the interplay between the two has not yet been explored in the context of SR.

Nd-chromite also appears to be a unique case in context of Nd sublattice magnetism. Below the ordering temperature of the M sublattice, the Nd-M interaction has a tendency to polarize the Nd sublattice following the M sublattice ordering, thus acting as an effective magnetic field. Evidence of this is observed in Nd nickelates, ferrites and chromites [25]. However, at sufficiently low temperature this coupling may compete with the weak R-R interaction and give rise to cooperative long range ordering in the Nd sublattice. While existence of Nd sublattice ordering has been established in fer-

rites [22], the stronger Nd-M interaction in chromites puts in doubt/questions the existence of a cooperative magnetic ordering for the Nd sublattice of these systems. This behavior is counter intuitive since the M sublattice ordering temperature is lower in chromites compared to ferrites.

All the above issues, make of $NdCrO_3$ a challenging and interesting system which still remains to be understood. In the present study, we investigate the spin reorientation phenomena in $NdCrO_3$ by considering a spin Hamiltonian which consists of isotropic $M^{3+}-M^{3+}$, $M^{3+}-R^{3+}$ and $R^{3+}-R^{3+}$ superexchange together with single-ion anisotropy of both Nd^{3+} and Cr^{3+} sites. We employ state-of-the-art first-principles density functional theory (DFT) calculations to extract the parameters of the spin Hamiltonian relevant for $NdCrO_3$. The parameters extracted from DFT calculations and based on the experimentally measured crystal structure of $NdCrO_3$ encode the structural and chemical details of the system. Subsequently, the finite temperature magnetic properties of the spin Hamiltonian was obtained by Monte-Carlo simulations considering the spin Hamiltonian. Our results reveal that such a Hamiltonian is able to capture the spin-reorientation in $NdCrO_3$ correctly. The calculated transition temperatures corresponding to the Néel ordering of Cr spins and SR are in reasonable agreement with experimental values. Our study pinpoints the interplay of the Nd-Cr interactions and single-ion anisotropy of Nd and Cr sites in driving this exceptional SR phenomena. Since we are primarily interested in the study of SR and in the role of single-ion anisotropy, this study does not take into account the anti-symmetric and the anisotropic-symmetric superexchange interactions, which would give rise to non-collinear magnetism of Cr spins resulting in a small canting, as reported experimentally.

Moreover, our first principles study combined with Monte-Carlo simulations unravel a yet unreported C-type magnetic ordering in the Nd sublattice, throwing further debate on the nature of cooperative ordering of Nd spins in $NdCrO_3$. Further experimental studies, as well as theoretical ones taking into account the influence of anti-symmetric and anisotropic-symmetric superexchange interactions are needed to settle the issue conclusively.

The present work underlines the effectiveness of first-principles calculations in capturing the complexity of rare earth transition metal oxides involved in the delicate balance between magnetic interactions and single ion anisotropies of two the magnetic sublattices. It further establishes the power of such approach in providing a microscopic understanding of SR transition in $NdCrO_3$, phenomenon that still remains unsolved by the theory.

COMPUTATIONAL DETAILS

Using the experimentally determined $Pbnm$ crystal structures, the symmetric exchange interactions between the magnetic ions, as well as their magnetic anisotropy parameters were estimated through the calculation of total energy

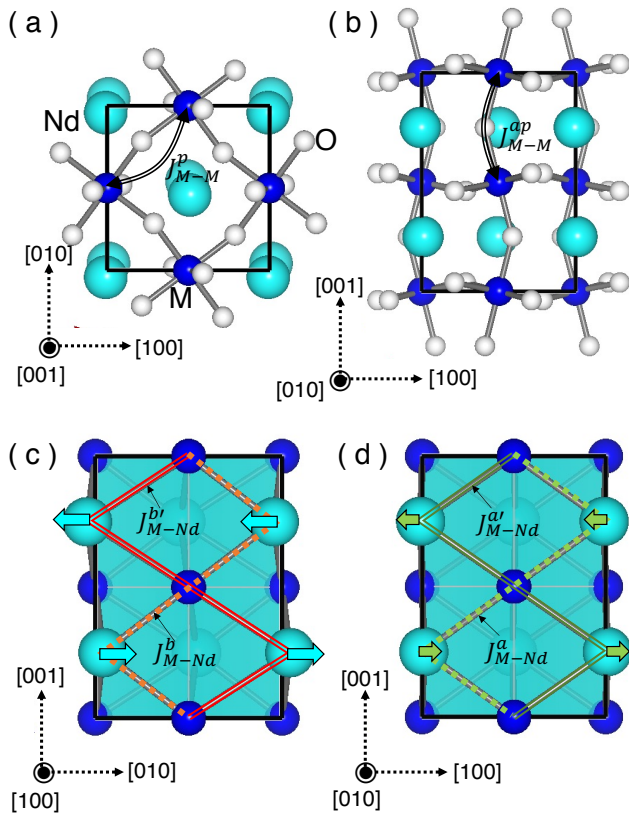


FIG. 1: Orthorhombic $Pbnm$ crystal structure of NdCrO_3 . Crystal structure showing the first nearest-neighbor isotropic M-M exchange interactions, in plane (J_{M-M}^p) (a) and out of plane (J_{M-M}^{ap}) (b). Crystal structure plot exhibiting four in-equivalent nn M-Nd exchange interactions, denoted as J_{M-Nd}^b and $J_{M-Nd}^{b'}$ (in the crystallographic bc plane) (c) & J_{M-Nd}^a and $J_{M-Nd}^{a'}$ (in the crystallographic ac plane) (d). The arrows indicate the anti-ferro off-centric displacements of Nd ions.

of various collinear magnetic configurations employing the density functional theory (DFT) based linearized augmented plane-wave (LAPW) method as implemented in the Wien2k code [26, 27]. We considered sixteen magnetic configurations in order to estimate the strength of the symmetric exchange interactions and six magnetic configurations to estimate the magnetic anisotropy parameters of the ions. We used the Perdew-Burke-Ernzerhof (PBE) [28] Generalized Gradient Approximation (GGA) form of exchange correlation functional. The effect of the missing correlation on the transition metal Cr sites (with localized $3d$ electrons) and rare earth Nd sites (with localized $4f$ electrons) beyond the GGA was taken into account through supplemented Hubbard U and Hund's coupling J_H terms using GGA+ U method [29]. The choice of appropriate U and J_H values, for that matter, is very crucial in quantitative description of the magnetic and electronic structures of strongly correlated insulators like the system in question. Following the values of U estimated by employing the constrained density functional theory (cDFT) method [30]

and previous theoretical studies [8, 31], we performed our calculations considering U for Cr in the range of 2 - 5.5 eV (0.15 - 0.40 Ryd). On the other hand, we set a 5.5 eV (0.40 Ryd) value of U at the Nd site. This strategy gave us the opportunity to study the effect of the relative strength of U at the Cr and Nd sites on the properties of NdCrO_3 . Additionally, we considered a range of values, 0 - 1.0 eV, for J_H parameter, a factor which is found to have a strong influence on the estimated magnetic parameters. We performed our calculations using a plane-wave cutoff of $RK_{MAX} = 7$ and Monkhorst-Pack Γ centred k -point mesh of $6 \times 6 \times 4$ for $Pbnm$ structure. We also considered $1 \times 2 \times 1$ and $2 \times 1 \times 1$ supercell structures to estimate R-M magnetic interactions and the corresponding k -point meshes were of the dimensions, $6 \times 4 \times 4$ and $4 \times 6 \times 4$, respectively.

Monte Carlo (MC) simulations were performed on an $8 \times 8 \times 8$ cell consisting of 4096 magnetic ions, and considering 10^9 MC steps for each temperature using the model Hamiltonian constructed through GGA+ U calculations. In Addition, we conducted finite temperature MC simulations further considering a wide variation in magnetic parameter range of R-M superexchanges, and single ion anisotropy of both R and M ions beyond the DFT estimated values, to unravel and identify the driving forces behind the complex magnetic behaviour of NdCrO_3 . In order to determine the primary collinear G-type AFM phase in the Cr sublattice, we calculated magnetic order parameter defined as

$$[m_a, m_b, m_c] = \langle \mathbf{S}_1 - \mathbf{S}_2 + \mathbf{S}_3 - \mathbf{S}_4 \rangle / 4S \quad (1)$$

where $\mathbf{S}_1 \rightarrow \mathbf{S}_4$ represent four Cr ($S = 3/2$) ions in the $Pbnm$ unit cell. m_a , m_b and m_c denote the staggered moments along the crystallographic a , b and c axis, respectively. We calculated specific heat as a function of temperature using,

$$C_v(T) = \frac{\langle \xi^2 \rangle - \langle \xi \rangle^2}{k_B T^2} \quad (2)$$

where the angles bracket denotes thermal average and ξ represents total energy of the system.

RESULTS

Crystal Structure

The NdCrO_3 compound crystallizes in orthorhombic $Pbnm$ space group, which is the GdFeO_3 -type distorted perovskite structure with both in-phase and out-of-phase CrO_6 octahedral tilting distortion pattern of $a^- a^- c^+$, as shown in Figure 1(a) and (b). The lattice constants of the orthorhombic unit cell were measured as [32], $a = 5.421 \text{ \AA}$, $b = 5.487 \text{ \AA}$ and $c = 7.694 \text{ \AA}$. The experimentally determined Wyckoff positions corresponding to Nd, Cr, O_{ap} (apical oxygen) and O_p (planar oxygen) ions are $4c$ ($x, y = -0.009, 0.042$), $4b$, $4c$ ($x, y = 0.089, 0.480$) and $8d$ ($x, y, z = -0.287, 0.285, 0.040$), respectively. The resultant orthorhombic distortion, measured

as $\frac{2 \times (b-a)}{(b+a)}$ is 0.012. In addition to rotation $a^0 a^0 c^+$ (M_3^+) and tilt $a^- a^- c^0$ (R_4^+) distortions, Nd ions exhibit anti-ferro off-centric displacements along the crystallographic a and b axes, following the R_5^+ (Figure 1(c)) and X_5^+ (Figure 1(d)) symmetries, respectively. This leads to the formation of Nd-Cr short bonds (3.165 Å and 2.293 Å) and long bonds (3.370 Å and 3.540 Å), respectively. We considered this crystal structure in order to conduct the first-principles electronic structure calculations and to construct the magnetic model Hamiltonian to perform finite temperature Monte Carlo simulations. Considering the fact that no significant change in orthorhombic distortion was reported below the Néel temperature (T_N) [32], we kept the crystal structure fixed in the temperature range of the Monte Carlo simulations.

Model Hamiltonian

To investigate the magnetic phase transitions in NdCrO₃ at finite temperatures we constructed a magnetic model Hamiltonian comprising of isotropic exchange interactions between the magnetic ions and the magnetic anisotropy energies of the magnetic ions. The isotropic exchange component of the Hamiltonian is given by,

$$H_{SE} = H_{M-M} + H_{M-Nd} + H_{Nd-Nd} \quad (3)$$

Where,

$$H_{M-M} = \sum_{ij} J_{M-M}^{ap} \mathbf{S}_i \cdot \mathbf{S}_j + \sum_{ij} J_{M-M}^p \mathbf{S}_i \cdot \mathbf{S}_j + \sum_{ij} J_{M-M}^{nnn} \mathbf{S}_i \cdot \mathbf{S}_j \quad (4)$$

represents the nearest neighbor (nn) isotropic exchange interactions between M spins (denoted by \mathbf{S}) mediated via apical (J_{M-M}^{ap}) and planar (J_{M-M}^p) oxygen (cf Figs 1(a) and 1(b)) and their next-nearest-neighbor (nnn) interactions (J_{M-M}^{nnn}).

The most important interactions are between two magnetic sublattices and the associated energy component is given by,

$$H_{M-Nd} = \sum_{ij} J_{M-Nd}^b \mathbf{S}_i \cdot \mathbf{S}'_j + \sum_{ij} J_{M-Nd}^{b'} \mathbf{S}_i \cdot \mathbf{S}'_j + \sum_{ij} J_{M-Nd}^a \mathbf{S}_i \cdot \mathbf{S}'_j + \sum_{ij} J_{M-Nd}^{a'} \mathbf{S}_i \cdot \mathbf{S}'_j \quad (5)$$

which incorporates the effect of the orthorhombic displacement of the Nd ions, resulting in four inequivalent exchange interactions; J_{M-Nd}^b , J_{M-Nd}^a , $J_{M-Nd}^{b'}$ and $J_{M-Nd}^{a'}$ (cf Figs. 1(c) and 1(d)). \mathbf{S}' denotes Nd spin. The first pair of interactions corresponding to the short Nd-Cr bond connections while the second pair represents the same along the longer Nd-Cr bonds. Here we define a parameter γ which denotes the strength of the strongest nn isotropic exchange interaction between two magnetic sublattices J_{M-Nd} relative to the

strongest exchange interaction between M spins J_{M-M} , i.e.

$$\gamma = \frac{J_{M-Nd}}{J_{M-M}}.$$

In addition, we considered the nn isotropic exchange interactions between the Nd spins along the three crystallographic axes, denoted as, J_{Nd-Nd}^a , J_{Nd-Nd}^b and J_{Nd-Nd}^c , respectively. The corresponding energy term is given by,

$$H_{Nd-Nd} = \sum_{ij} J_{Nd-Nd}^a \mathbf{S}'_i \cdot \mathbf{S}'_j + \sum_{ij} J_{Nd-Nd}^b \mathbf{S}'_i \cdot \mathbf{S}'_j + \sum_{ij} J_{Nd-Nd}^c \mathbf{S}'_i \cdot \mathbf{S}'_j \quad (6)$$

The magnetic anisotropy of the system was modelled by considering the single ion anisotropy (SIA) energies of the M and Nd ions. The corresponding component of the spin Hamiltonian is given by,

$$H_{SIA} = \sum_i \{ E_M (S_{ix}^2 - S_{iy}^2) + D_M S_{iz}^2 \} + \sum_i [E_{Nd} \{ (S'_{ix})^2 - (S'_{iy})^2 \} + D_{Nd} (S'_{iz})^2] \quad (7)$$

The x , y and z directions correspond to the crystallographic a , b and c axes, respectively, of the $Pbnm$ structure. For ($E < 0, D < 0, |E| > |D|$) and ($E < 0, D > 0$) conditions, the spins tend to orient along the x (crystallographic a) axis. On the other hand, ($E < 0, D < 0, |E| < |D|$) and ($E > 0, D < 0, |E| < |D|$) denote the preference of spins to orient along z (crystallographic c) axis. Finally, ($E > 0, D < 0, |E| > |D|$) and ($E > 0, D > 0$) tend to orient the spins along y (crystallographic b) axis. The analysis based on site symmetries of both Cr and Nd ions shows the possible existence of non-zero off-diagonal components of the associated SIA tensors in addition to the non-zero diagonal components. However, in the present study, we have taken only the latter into consideration.

DFT Electronic structure

Figure 2(a) shows the electronic structure of NdCrO₃ computed within GGA+ U formalism and considering a G-type antiferromagnetic order in both the Nd and Cr sublattice. The results presented in the following are for the choice of $U_{Cr} = 2.2$ eV, $U_{Nd} = 5.5$ eV and $J_H = 0.3$ eV, which were found to provide best description of magnetic moments and exchange interactions vis-à-vis the experimental observations. The system shows insulating behavior with ~ 2.5 eV band gap. The approximate octahedral oxygen environment surrounding Cr ions splits the $3d$ states into t_{2g} and e_g manifolds. The t_{2g} manifold is filled (empty) in the majority (minority) spin channel for Cr, indicating a nominal 3+ valence state as reported in orthochromites. The electron occupancy of the Nd - $4f$ orbitals also indicates a 3+ valence state. The values of the calculated spin moments at Cr and Nd sites are $\sim 2.52 \mu_B$ and $\sim 2.96 \mu_B$, respectively. These spin moments provide

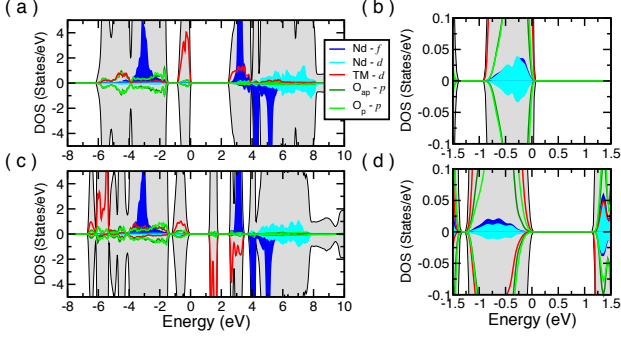


FIG. 2: (a) and (c) Calculated density of states (DOS) for NdCrO_3 and NdFeO_3 considering collinear G-type antiferromagnetic order in Cr sublattice as well as Nd sublattice. The Nd-Cr and Nd-Fe hybridization are highlighted in zoomed plot (b) and (d). We considered $U = 2.2$ eV and $J_H = 0.3$ eV for Cr $3d$ states and $U = 4.5$ eV and $J_H = 0.3$ eV for Fe $3d$ states. A higher U value of 5.5 eV and $J_H = 0.3$ eV for Nd $4f$ states was used.

TABLE I: Estimated values of isotropic exchange interactions and SIA parameters using $U=2.2$ eV and 5.5 eV for the transition metal Cr $3d$, and rare-earth $4f$ states, respectively, and $J_H = 0.3$ eV.

Isotropic Exchange (meV)							
System	J_{M-M}^p	J_{M-M}^{ap}	J_{M-M}^{nnn}	J_{M-Nd}^b	J_{M-Nd}^{bt}	J_{M-Nd}^a	J_{M-Nd}^{at}
NdCrO_3	4.66	6.01	0.09	2.63	-2.08	0.84	-0.23

SIA (meV)					
System	E_{Nd}	D_{Nd}	E_M	D_M	
NdCrO_3	-0.40	-0.10	0.003	-0.01	

additional support to the nominal 3+ valences at both transition metal (M) and rare-earth (R) sites. The $4f$ electrons of Nd are coupled with its $5d$ electrons by the intra-atomic exchange interaction. Also, since the $5d$ orbitals are spatially extended, they hybridize with the M - $3d$. This hybridization has been clearly depicted in the zoomed plot in Figure 2(b), which shows a strong overlap between the Nd- $5d$ - $4f$ and the Cr - $3d$ states. For comparative analysis, we also calculated the electronic structure of the G-type ordered magnetic phase of NdFeO_3 considering $U = 4.5$ eV and $J_H = 0.3$ eV at the Fe $3d$ states, presented in Fig. 2(c) and (d). As in the case of orthochromites, in this orthoferrite too, both Fe and Nd ions tend to favor the formation of +3 valence state. Very interestingly, we find that the integrated DOS of Nd- $5d$ in the energy range of -1.5 eV to Fermi level is approximately 2 times higher in NdCrO_3 compared to that in NdFeO_3 , which indicates that the Nd-Cr hybridization is about 2 times stronger than the Nd-Fe hybridization. This relation is in good line with the experimentally observed relation (based on the specific heat and neutron-diffraction measurements [16] between the values of the mean-field Nd-Cr and Nd-Fe interaction parameters (n_{M-R}), where the former is 2.6 times as that of the latter.

Estimated Isotropic Exchange Interactions

We estimated the values of the isotropic exchange interactions between magnetic ions of NdCrO_3 using the calculated total energies of sixteen spin configurations and the results are listed in Table I for $J_H = 0.3$ eV and the U value of 2.2 eV and 5.5 eV corresponding to the Cr $3d$ and Nd $4f$ states, respectively. Additionally, we conducted the calculations considering a range of U and J_H values. The results are summarized in the Supplementary Fig. S1 and S2. We estimated the values of exchange interactions considering spin value of $3/2$ for both Cr and Nd. The strongest interaction, $J_{Cr-Cr} = 6.01$ meV, corresponds to the antiferromagnetic (AFM) nn interaction between Cr spins mediated via the apical oxygens. The Cr spins are also coupled antiferromagnetically in the ab plane, leading to the stabilization of the G-type AFM phase, which is in agreement with the experimental observations [3]. The nnn interactions are comparatively weak and AFM in nature with an average value of ~ 0.09 meV, which is expected to cause weak magnetic frustration in the Cr sublattice. The values of the nn exchange interactions increase linearly with the increase of J_H (see Supplementary Fig. S1(a)).

The interactions between two magnetic sublattices significantly vary with the value of J_H , as shown in the Supplementary Fig. S1(b). The orthorhombic distortions result in AFM and FM interactions between the Nd and Cr spins along the shorter and longer bond directions, respectively. We observe that $|J_{Cr-Nd}^b - J_{Cr-Nd}^{bt}| > |J_{Cr-Nd}^a - J_{Cr-Nd}^{at}|$, implying that the difference in magnetic interactions due to anti-ferro off-centric displacements of Nd ions along crystallographic b axis is higher than that along the crystallographic a axis. Interestingly, the displacement of the Nd ions along b axis (Q_b) is higher in order of magnitude compared to that along the a axis (Q_a). Thus, the orthorhombic separation between magnetic interactions directly vary with the amplitude of the off-center displacement of the Nd ions. The strongest interaction corresponds to AFM $J_{Cr-Nd} = J_{Cr-Nd}^b = 2.63$ meV which gives rise to the relative strength of $\gamma = 0.44$. This relative strength varies from 0.25 - 0.89 as we vary the J_H value from 0 to 1.0 eV (see Supplementary Fig. S2). This indicates a strong correlation between the exchange interactions between the two magnetic sublattice and J_H . The average exchange interaction (J_{Cr-Nd}^{avg}) between two magnetic sublattices is AFM in nature, which is in line with the experimental observation [19]. It is important to point out here, that a similar exercise carried out for NdFeO_3 with $U = 4.5$ eV and $J_H = 0.3$ eV at the Fe site, gave a γ value of 0.25, a factor of 1.8 smaller compared to NdCrO_3 , in good agreement with our conclusions on relative Nd-M hybridization between chromites and ferrites from density of states as well as that concluded from specific heat measurement [16].

In addition, we also estimated the magnetic interactions between Nd spins, which were found to be weak and AFM in nature along all three crystallographic axes with an average value of 0.02 meV, indicating a G-type magnetic order in the

Nd sublattice. However, these interactions are of order of magnitude weaker than the magnetic interactions between two sublattices.

Estimated Single Ion Anisotropy (SIA)

Next, we calculated the magnetic anisotropy energy of the Nd ions, and the results are given in Table I. In order to decouple the contribution of the Cr spin sublattice, we only employ Spin-Orbit (LS) coupling at the Nd spins. As the electronic configuration of R-4*f* electrons follows Hund's rule, the orbital magnetic moment appears in the presence of spin-orbit coupling (SOC). Once the direction of the 4*f* orbital moment gets fixed, the direction of the spin moment also gets fixed by the LS coupling. The anisotropy energies were calculated by considering spin configurations oriented along the crystallographic *a* (*x*), *b* (*y*) and *c* (*z*) axes. We observed that, irrespective of the value of J_H , the anisotropy energy associated with the orientation of Nd spins along the crystallographic *b* axis is higher than the corresponding energies along the crystallographic *a* and *c* axes (See Supplementary Fig. S3(a)). Our calculations show that the Nd sublattice exhibit biaxial magnetic anisotropy, where the easy and intermediate magnetic axes are along the crystallographic *a* and *c* axes, respectively and the magnetic hard axis is along the crystallographic *b* axis (see Table I and Supplementary Fig. S3(a)). The calculated orbital moment of Nd $\sim 1.63 \mu_B$ and is oriented antiparallel to the spin moment. The net magnetic moment $\mu_{Nd} \sim 1.33 \mu_B$, lying well within the experimentally reported range of 1.30-1.93 μ_B [33, 34]. We notice here $J_{Cr-Nd}^{avg} = 0.29$ meV, comparable to DFT estimated SIA of Nd spins, hinting into a strong interplay between the two.

Compared to the magnetic anisotropy energies of the Nd ions, the anisotropy energies of the Cr ions are order of magnitude lower. To obtain the magnetic anisotropy of the Cr ions, we switch on the LS coupling only for the Cr ions. The computed orbital moment at the Cr site $\sim 0.03 \mu_B$. As shown in the Supplementary Fig. S3(b), Cr tends to orient along the crystallographic *c* axis and this tendency enhances with the increase in J_H . This observation agrees with the experimentally observed stabilization of the G_z magnetic phase below Néel temperature [19]. However, the weak magnetic anisotropy of the Cr spins is expected to be associated with high numerical error. We, therefore, scan the stability of the magnetic phases in NdCrO₃ as a function of the SIA parameters of the Cr spins (E_{Cr} , D_{Cr}) employing finite temperature Monte Carlo simulations.

Finite temperature Monte Carlo Simulations

Monte Carlo (MC) simulations were performed using the model Hamiltonian constructed with the U values of 2.2 eV and 5.5 eV at the Cr 3*d* and Nd 4*f* states, respectively and $J_H = 0.3$ eV. This set of particular values of U and J_H

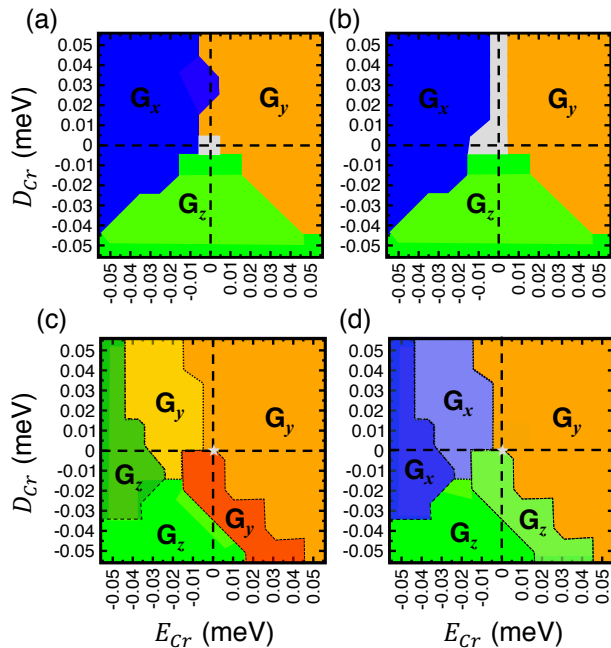


FIG. 3: Observed collective spin ordering in the Cr sublattice at 5 K (a) and 75 K (b) as a function of E_{Cr} and D_{Cr} for $|E_{Nd}| = |D_{Nd}| = 0$. The same for GGA+U estimated values of E_{Nd} and D_{Nd} at 5 K (c) and 75 K (d). G_x , G_y and G_z denote orientation of Cr spins along the crystallographic *a*, *b* and *c* axes, respectively. Different phases are shaded with different colors. The color coding is same between 5 K and 75 K, if there is no change in symmetry of spin ordering of Cr spins and shaded differently when there is a change in symmetry of spin ordering of Cr spins between 5 K and 75 K. The values of isotropic magnetic exchanges are kept fixed at GGA+U estimated values obtained with choice of $J_H = 0.3$ eV. Within the parameter region shaded with light grey, none of the following phases, G_x , G_y and G_z , are formed.

were taken into consideration, since the magnetic properties of the material, when calculated using this particular set, were in best agreement with the experimentally obtained results [15, 16, 19]. The primary motivation of the present study is to explore the interplay between isotropic Nd-Cr exchange interactions and SIA which can induce the spin-reorientation transitions. With this motivation in mind, we first explore the parameter space of SIA, (E_{Nd}, D_{Nd}) and (E_{Cr}, D_{Cr}) .

Case: $E_{Nd} = D_{Nd} = 0$. We start our discussion by considering the MC simulation results where the magnetic anisotropy of the Nd ions is switched off ($E_{Nd} = D_{Nd} = 0$) and the magnetic anisotropy of Cr ions is varied from -0.05 to 0.05 meV. Figure 3(a) and (b) show the observed magnetic order in the Cr sublattice at 5 K and 75 K, respectively, as a function of E_{Cr} and D_{Cr} . We determined the order by calculating the staggered magnetization as defined in Eq. 1. Irrespective of the value of E_{Cr} and D_{Cr} , the specific heat, calculated as a function of temperature shows a peak at around 172 K, indicating a magnetic transition from the paramagnetic phase to a G-type AFM phase in the Cr sublattice and a disordered state in the Nd sublattice. Depending on the parameter values

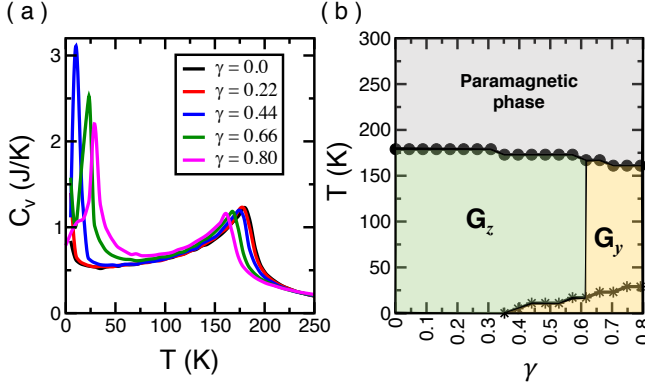


FIG. 4: (a) Calculated temperature dependence of specific heat for a choice of γ values. We used $E_{Cr} = 0.02$ meV and $D_{Cr} = -0.05$ meV. Though the nature of magnetic phase transitions strongly depend on the magnetic anisotropy of Nd and Cr ions, the value of transition temperatures shows weak dependence. (b) Magnetic phase diagram in T - γ plane, demarcating the paramagnetic, G_z and G_y spin-ordered phases of Cr sublattice. The calculated Néel temperature T_N values, plotted in solid circles, denote paramagnetic to G-type AFM ordering temperature, while the second transition temperature is plotted in stars. For $\gamma \sim 0.35 - 0.62$, stars denote $G_z \rightarrow G_y$ SR transition.

of E_{Cr} and D_{Cr} , G_x or G_y or G_z phase is stabilized in Cr sublattice. Comparison between Figure 3(a) and (b) reveals no spin-reorientation transition of the Cr spins was observed down to 5K. This provides the key finding of our study that for SR in Cr sublattice the SIA of Nd ions plays a crucial role.

Case: $E_{Nd} \neq 0$, $D_{Nd} \neq 0$. Figure 3(c) and (d) summarizes the results of MC simulations considering the DFT estimated values of SIA E_{Nd} and D_{Nd} parameters (see Table I). The main findings are as follows; (1) The calculated specific heat for a temperature range of 300-5 K, shows two peaks. One at around 172 K and another at around 11 K. The first transition temperature corresponds to Néel temperature (T_N) forming G-type Cr spin order. T_N value remained unchanged between $E_{Nd} = D_{Nd} = 0$, and $E_{Nd} \neq 0$, $D_{Nd} \neq 0$, indicating that high temperature magnetic ordering of Cr sublattice does not depend on Nd sublattice. However, contrary to $E_{Nd} = D_{Nd} = 0$ case, SR transition is observed in Cr sublattice depending on the choice of E_{Cr} , D_{Cr} (compare Figure 3(c) and (d)). The existence and precise nature of the SR transition is found to strongly depend on the value of Cr SIA parameters, as depicted in various shaded regions in Figure 3(c) and (d). (2) For the choice of (E_{Cr} , D_{Cr}) parameters within a critical range, as shown by the region shaded in red in Figure 3(c), a reorientation of the G-type ordered Cr spins from z to y axis ($G_z \rightarrow G_y$) at 11 K is observed, which corresponds to the experimentally reported spin reorientation transition observed in NdCrO_3 [16]. (3) Additionally, our results highlight a comprehensive correlation between the magnetic anisotropy of the magnetic ions and the nature of SR transitions in the Cr sublattice. The Cr spins, notably, either orient along the y or the z axis, below the second magnetic transition temperature.

The strong tendency of the Nd spins to be oriented along the x axis, exclude the formation of G_x magnetic phase.

The DFT estimated SIA coefficients of Cr ions are, $E_{Cr} = 0.003$ meV and $D_{Cr} = -0.01$ meV, which lie in the critical parameter space that leads to the $G_z \rightarrow G_y$ spin-reorientation transition at the second transition temperature. Two noteworthy points in this regard are, (I) the $G_z \rightarrow G_y$ SR transition takes place for $D_{Cr} < 0$, *i.e.* when the magnetic easy axis of the Cr sublattice is along the crystallographic c axis, which is in line with the observed trend of magnetic anisotropy of Cr ions through DFT calculations, and (II) based on our present mechanism, SR transitions occur if the magnetic easy axis of Cr sublattice coincides with one of the easy axes of Nd sublattice and due to the strong Cr-Nd superexchange interactions below SR transition temperature (T_{SR}) Cr spin orient along the magnetic hard axis of Nd sublattice. The calculated T_N and T_{SR} (see Figure 4(a)) are in same ball park but somewhat underestimated compared to the experimentally reported values of 224 K and 34 K [16], respectively. The present model, however, excludes the effect of anisotropic and anti-symmetric exchange interactions, which can influence the precise values of the magnetic transition temperatures. The magnetic exchanges and SIA being strongly dependent on choice of J_H value provides another avenue of fine tuning of the transition temperatures, which we refrain from doing as our motivation is to unravel the origin rather than providing a perfect matching with experimental transition temperatures.

In order to further explore the correlation between the relative strength of the exchange interactions between the two magnetic sublattices and the SR transitions, we carried out additional MC simulations as a function of γ keeping the DFT determined relative strength of all four Cr-Nd interactions fixed. The $\gamma \sim 0.44$ case corresponds to the DFT estimated parameters. The calculated Cr sublattice staggered magnetization as a function of γ is shown in Supplementary Fig. S4(b). Our results demonstrate existence of a second transition only above a critical value of $\gamma = 0.35$, as shown in Figure 4(a). While the value of Néel temperature decreases with the increase of γ , the value of second transition temperature increases. As shown in the $\gamma - T$ phase diagram in Figure 4(b) and Supplementary Fig. S4(b), within a range of $\gamma \sim 0.35 - 0.62$, NdCrO_3 is found to show $G_z \rightarrow G_y$ SR transition. For $\gamma > 0.62$, the second transition corresponds to the spin ordering in the Nd sublattice, and not to SR transition of Cr sublattice.

The above exercise conclusively establishes that the SR transition of NdCrO_3 is a complex interplay of Nd-Cr magnetic exchanges, SIA of Nd and Cr sublattice.

Magnetic ordering in Nd sublattice

So far, we have discussed the collective magnetic ordering in the Cr sublattice as observed at different temperatures. In this subsection we take up the case of Nd sublattice.

The nature of the magnetic ordering corresponding to the

Nd sublattice till date remains ambiguous [16, 19, 22]. The very existence of magnetic ordering in Nd sublattice, as a matter of fact, is debated, given the fact the ordering must occur at very low temperature due to weak Nd-Nd interaction. The evidence of ordering of R sublattice is normally manifested as a small λ peak in specific heat superimposed on Schottky anomaly, the latter arising due to finite R-M interaction. In contrast to Nd ferrite, no such λ peak is observed in the specific heat of NdCrO_3 suggesting cooperative ordering of Nd sublattice is prohibited [22]. Neutron diffraction study [19] on the other hand, suggest C-type magnetic ordering in Nd sublattices, where Nd spins are ordered in AFM and FM manners in the crystallographic (001) plane and along the crystallographic [001] axis, respectively (see Fig. 5(a)). We denote this magnetic structure as C_{001} . However, our MC results below T_{SR} , show the stabilization of a different variety of C-type ordering. Here, the Nd spins form AFM ordered patterns along the crystallographic [001] and [1-10] axes and FM ordered pattern along the crystallographic [110] axis. We observe that the Nd spins are directed along [100] axis (x axis) (cf Fig. 5(b)). We denote this magnetic ordering as C_{110} . This type of magnetic ordering is expected to break the crystal symmetry, leading to doubling of the size of the unit cell.

We though need to keep few points in mind. The strong isotropic exchange interactions between two magnetic sublattices create C_{110} type canted spin component in the Cr sublattice. Below T_{SR} the magnetically ordered Cr sublattice is expected to create a strong anisotropic and anti-symmetric exchange field on the Nd spin. This field can compete with the SIA tendency, and can influence the precise nature of spin ordering of Nd sublattice. Our present calculation does not take into account these additional factors which may influence the magnetic order in the Nd sublattice at low temperatures, leaving the issue open. Further investigations need to be conducted to gain a deeper insight in this regard.

CONCLUSION & DISCUSSIONS

Using combination of first-principles calculations and finite-temperature MC simulations on DFT derived spin Hamiltonian we studied the complex magnetism of NdCrO_3 , especially the spin reorientation transition of Cr sublattice. The most exhaustive theoretical study on spin reorientation in rare-earth orthochromites and orthoferrites [12], given about three decades ago, was based on mean field study of the spin Hamiltonian in parameter space. While this study was successful in explaining SR of both category (I) and (II), it failed to explain SR of category (V) *i.e.* that of NdCrO_3 motivating the present study. Our study importantly took into account the SIA of Nd spins, which was neglected in the study by Yamaguchi [12]. In order to gain understanding on the microscopic origin of SR transition in NdCrO_3 , we carried out calculations switching off and on SIA of Nd spins, varying the SIA of Cr spins around the DFT estimated values, and varying the Nd-Cr exchange strength, parameterized through γ .

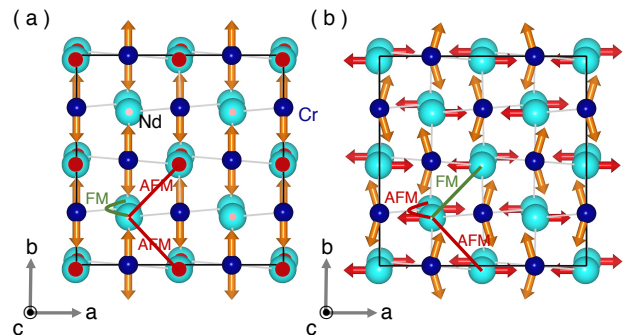


FIG. 5: (a) Experimentally proposed C-type magnetic ordering in the Nd sublattice [19] having $Pbnm$ magnetic symmetry. Nd spins (denoted by red arrow) orient along z axis. The Nd spins order in AFM and FM patterns in the (001) plane and along the [001] axis, respectively. We denote this magnetic ordering as C_{001} . (b) Proposed C-type magnetic ordering in the Nd sublattice through the MC simulations. Nd spins are oriented along x axis. The Nd spins form AFM ordering along the [001] and [1-10] axes and FM ordering along [110] axis. We denote this magnetic ordering as C_{110} . The Cr spins (denoted by orange arrow) are ordered in G_y pattern. The strong isotropic exchange interactions between two magnetic sublattices create C_{110} type canted spin component in the Cr sublattice.

Our analysis established the crucial role of SIA of Nd spins in driving the SR transition, provided the Nd-Cr magnetic exchange is above a critical strength. Strengthening of Nd-Cr exchange further beyond another limit leads to cooperative ordering of Nd sublattice avoiding the SR transition of Cr sublattice. Furthermore, the experimentally observed nature of SR transition in NdCrO_3 was found to be reproduced only for a restricted parameter range of SIA of Cr spins, highlighting of importance of SIA of Cr spins, though it is order of magnitude weaker in strength compared to SIA of Nd spins. Thus, our findings point to the fact that SR observed in NdCrO_3 arises out of delicate balance between Nd-Cr exchange, Nd SIA as well as Cr SIA. While the significant strength of Nd-Cr exchange and SIA of Nd spins set the stage, the SIA of Cr spins which is an order of magnitude smaller compared to that of Nd spins, decides the details.

We would like to end our discussion with some open issues and suggestions. Our study as mentioned already did not take into account the anti-symmetric and anisotropic-symmetric exchange interactions, rather focused only on isotropic exchanges. The anti-symmetric and anisotropic-symmetric exchanges in M sublattice are expected to give rise to canting and ferromagnetic component to Cr spin ordering, as observed experimentally. These exchanges between M and R sublattices were suggested to be crucial for driving SR in GdCrO_3 for example, though they are expected to be one and two orders of magnitude smaller compared to isotropic exchanges. We note the importance of SIA is negligible for Gd^{3+} thus making the anti-symmetric exchange of M-R interaction important. In case of NdCrO_3 , however, consideration of only the isotropic M-R exchange in presence of finite, and mod-

erately strong SIA of Nd spins, together with weak but finite SIA of Cr spins, was sufficient to capture the SR. The effect of anti-symmetric and anisotropic-symmetric exchange interactions, thus would come as secondary effect.

While our study primarily focused on SR transition, we also studied the possibility of cooperative ordering of Nd spins, which remains controversial. Our study points to a C_{110} type ordering of Nd spins, in contrast to C_{001} type ordering suggested from neutron diffraction [19]. This will be taken up in a future study involving a more complete Hamiltonian. Also it calls for further experimental studies.

Finally, it will be an interesting idea to study the SR in mixed orthoferrite-chromite compound, $\text{NdFe}_x\text{Cr}_{1-x}\text{O}_3$, given the fact that γ is about a factor of two smaller in NdFeO_3 compared to NdCrO_3 , while the SIA of Fe is expected to be smaller compared to Cr due to its suppressed orbital degeneracy. This may make the influence of the anti-symmetric and anisotropic-symmetric exchange interactions important. It is interesting to note that both the high temperature and the low temperature symmetry of the spin ordering of M sublattice in NdFeO_3 is different from that of NdCrO_3 , it being G_x (G_z) for NdFeO_3 and G_z (G_y) for NdCrO_3 before (after) SR. To the best of our knowledge, the phase diagram of mixed compound, $\text{NdFe}_x\text{Cr}_{1-x}\text{O}_3$ is yet to be explored either experimentally or theoretically. We hope our study will motivate further studies in this direction.

ACKNOWLEDGEMENTS

The authors gratefully acknowledge discussion with Badiur Rahaman, Sudipta Bandyopadhyay and Sourav Kanthal. Research at Tokyo Institute of Technology is supported by the Grant-in- Aid for Scientific Research 19K05246 and 19H05625 from the Japan Society for the Promotion of Science (JSPS). HD acknowledges computational support from TSUBAME supercomputing facility. TS-D acknowledges J.C.Bose National Fellowship (grant no.JCB/2020/000004) for funding.

* Electronic address: das.h.aa@m.titech.ac.jp

- [1] D. Treves, Phys. Rev. 125, 1843 (1962).
- [2] K. W. Blazey and G. Burns, Proc. Phys. Soc. **91**, 640 (1967).
- [3] K. Tsushima, K. Aoyagi and S. Sugano, J. appl. Phys. **41**, 1238 (1970).
- [4] R. L. White, J. Appl. Phys. **40**, 1061 (1969).
- [5] Y. Tokunaga, S. Iguchi, T. Arima, and Y. Tokura, Phys. Rev. Lett. **101**, 097205 (2008).
- [6] B. Rajeswaran, D. I. Khomskii, A. K. Zvezdin, C. N. R. Rao, and A. Sundaresan, Phys. Rev. B **86**, 214409 (2012).
- [7] Y. Tokunaga, N. Furukawa, H. Sakai, Y. Taguchi, T. Arima and Y. Tokura, Nat. Mater. **8**, 558–562 (2009).
- [8] H. J. Zhao, L. Bellaiche, X. M. Chen and J. Íñiguez, Nat. Commun. **8**, 14025 (2017).
- [9] X. Ye, J. Zhao, H. Das, D. Sheptyakov, J. Yang, Y. Sakai, H. Hojo, Z. Liu, L. Zhou, L. Cao, T. Nishikubo, S. Wakazaki, C. Dong, X. Wang, Z. Hu, H.-J. Lin, C.-T. Chen, C. Sahle, A. Efiminko, H. Cao, S. Calder, K. Mibu, M. Kenzelmann, L. H. Tjeng, R. Yu, M. Azuma, C. Jin and Y. Long, Nat. Commun. **12**, 1917 (2021).
- [10] M. Marezio, J. P. Remeika and P. D. Dernier, Acta Cryst. **B26**, 2008-2022 (1970).
- [11] M. C. Weber, J. Kreisel, P. A. Thomas, M. Newton, K. Sardar, and R. I. Walton, Phys. Rev. B **85**, 054303 (2012).
- [12] T. Yamaguchi, J. Phys. Chem. Solids. **35**, 479 (1974).
- [13] E. Bousquet and A. Cano, J. Phys.: Condens. Matter **28**, 123001 (2016).
- [14] D. Treves, J. Appl. Phys. **36**, 1033 (1965).
- [15] E. F. Bertaut, J. Mareschal, G. de Vries, R. Aleonard, R. Pauthenet, J. P. Rebouillat, and J. Sivardiere, IEEE Trans. Magn. **2**, 453 (1966).
- [16] F. Bartolomé, J. Bartolomé, M. Castro, and J. J. Meleró, Phys. Rev. B **62**, 1058 (2000).
- [17] I. Dzialoshinski, J. Phys. Chem. Solids **4**, 241 (1958).
- [18] T. Moriya, Phys. Rev. **120**, 91 (1960); In: *Magnetism I* (Edited by G. T. Rado and H. Suhl), p. 85. Academic Press, New York (1963).
- [19] N. Shamir, H. Shaked, S. Shtrikman, Phys. Rev. B **24**, 6642 (1981).
- [20] E. F. Bertaut and J. Mareschal, Solid. Stat. Commun., **5**, 93, (1967).
- [21] R. M. Hornreich, Y. Komet, R. Nolan, B. M. Wanklyn, I. Yaeger, Phys. Rev. B **12**, 5094 (1975).
- [22] F. Bartolomé, M. D. Kuzmin, J. Bartolomé, J. Blasco, J. García, and F. Sapiña, Solid State Commun. **91**, 177 (1994).
- [23] J.Ramesh, N.Raju, S.Shraavan Kumar Reddy, M.Sreenath Reddy, Ch.Gopal Reddy, P.Yadagiri Reddy, K.Rama Reddy, V.Raghavendra Reddy, J. Alloy Compounds, **711** 300 (2017).
- [24] R.M. Hornreich, J. Magn. Mater. **7** 280 (1978).
- [25] J. B. Ayasse, A. Berton, and J. Sivardiere, C. R. Seances Acad. Sci., Ser. B **271**, 1220 (1970).
- [26] P. Blaha, K. Schwarz, G. K. H. Madsen, D. Kvasnicka, J. Luitz, R. Laskowski, F. Tran and L. D. Marks, WIEN2k: An Augmented Plane Wave plus Local Orbitals Program for Calculating Crystal Properties; Vienna University of Technology: Austria, 2018 <http://www.wien2k.at/index.html>.
- [27] P. Blaha, K.Schwarz, F. Tran, R. Laskowski, G.K.H. Madsen and L.D. Marks, J. Chem. Phys. **152**, 074101 (2020).
- [28] J. P. Perdew, K. Burke, and M. Ernzerhof, Phys. Rev. Lett. **77**, 3865 (1996).
- [29] V. I. Anisimov, I. V. Solovyev, M. A. Korotin, M. T. Czyżyk, and G. A. Sawatzky, Phys. Rev. B, **48**, 16929 (1993).
- [30] P. Dederichs, S. Blügel, R. Zeller, H. Akai, Phys. Rev. Lett. **53**, 2512 (1984).
- [31] V. I. Anisimov, J. Zaanen, and O. K. Andersen, Phys. Rev. B **44**, 943 (1991); W. E. Pickett, S. C. Erwin, and E. C. Ethridge Phys. Rev. B **58**, 1201 (1998).
- [32] J. Prado-Gonjal, R. Schmidt, J.-J. Romero, D. Ávila, U. Amador, and E. Morán, Inorg. Chem. **52**, 1, 313–320 (2013).
- [33] E. F. Bertaut and J. Mareschal, Solid State Commun. **5**, 93 (1967).
- [34] N. Shamir, H. Shaked, and S. Shtrikman, Phys. Rev. B **24**, 6642 (1981).

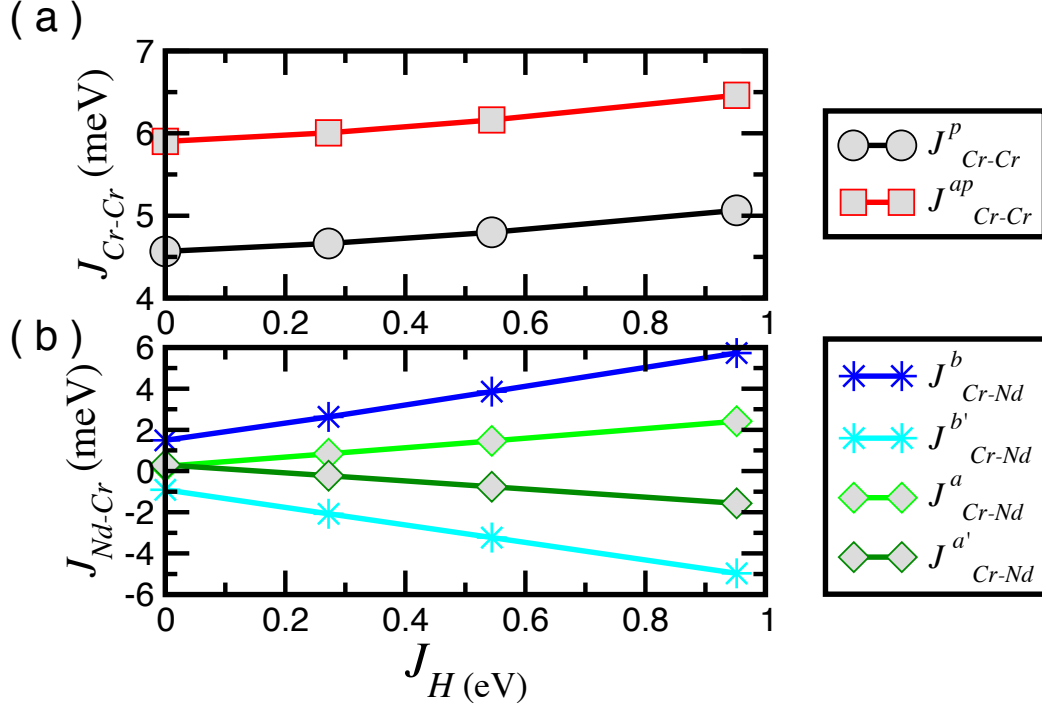


FIG. S1: Calculated superexchange interactions between Cr spins (a) and Cr and Nd spins (b) as a function of J_H . We present the results for the U value of 2.2 eV and 5.5 eV at Cr 3d and Nd 4f site, respectively.

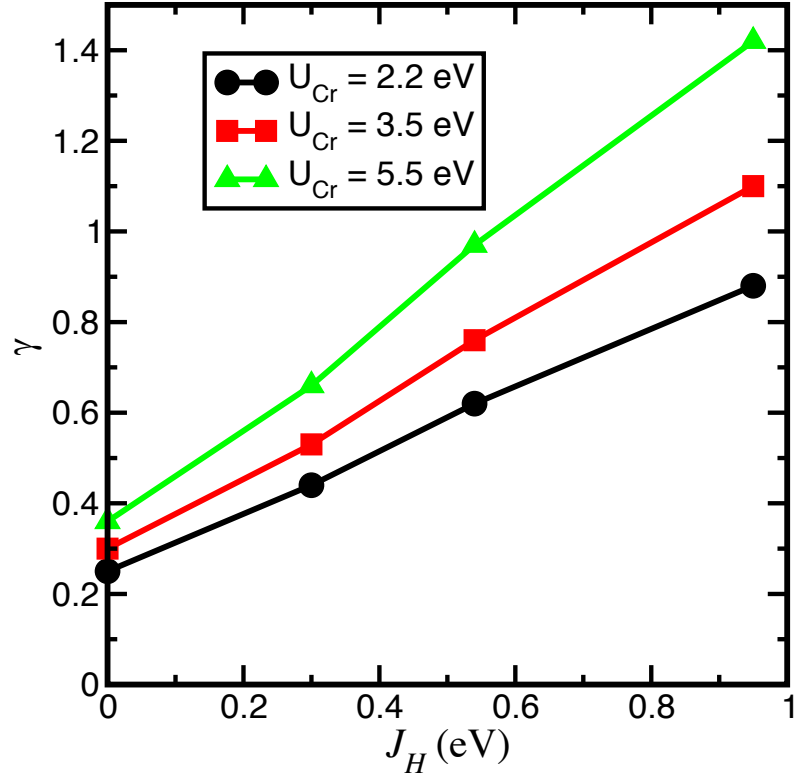


FIG. S2: Estimated relative strength of Cr-Nd magnetic interaction with respect to Cr-Cr magnetic interaction, which is denoted as γ , as a function of J_H and U value of Cr. We used $U = 5.5$ eV value for Nd $4f$ site.

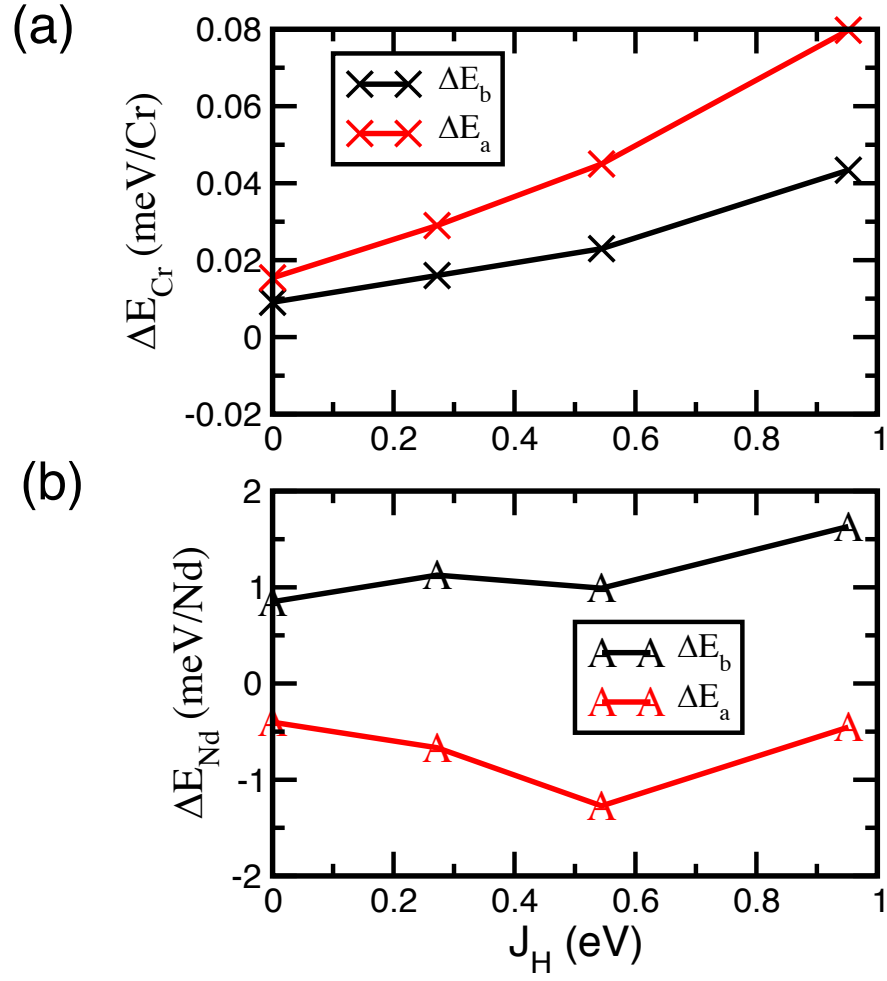


FIG. S3: Calculated relative magnetic anisotropy energies (MAE) for the Cr (a) and Nd (b) ions, as a function of J_H . The relative MAE are defined as, $\Delta E_b = E_b - E_c$ and $\Delta E_a = E_a - E_c$. Where E_a , E_b and E_c denote total energy corresponding to the spin orientation along crystallographic a , b and c axes, respectively. We present the results for the U value of 2.2 eV and 5.5 eV at Cr $3d$ and Nd $4f$ site, respectively.

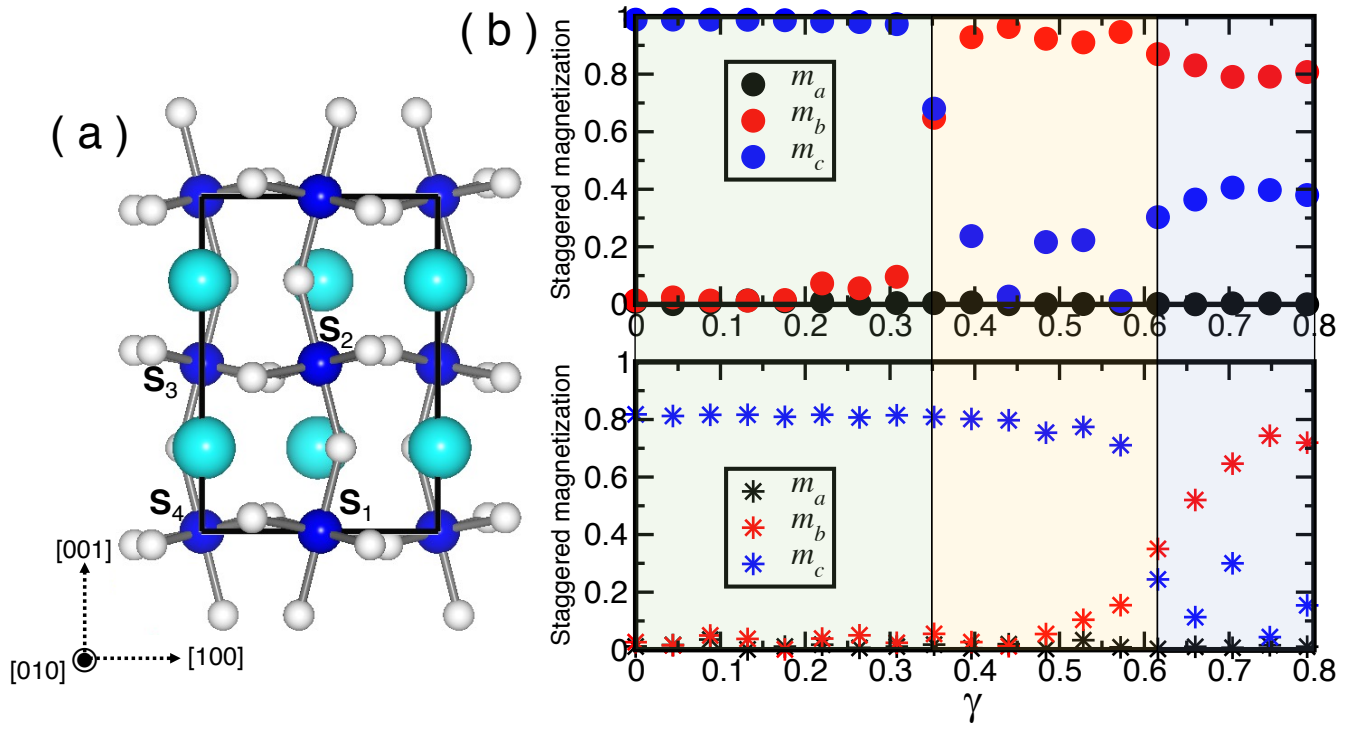


FIG. S4: (a) $Pbnm$ crystal structure and the Cr spins are denoted as $S_1 \rightarrow S_4$. (b) Calculated staggered magnetization at 5 K (upper panel) and 75 K (lower panel) as a function of γ .